Inclusion complexes of EMPO derivatives with 2,6-di-*O*-methyl-β-cyclodextrin: synthesis, NMR and EPR investigations for enhanced superoxide detection†

David Bardelang,[a] Antal Rockenbauer,[b] Hakim Karoui,[a] Jean-Pierre Finet,*[a] Inga Biskupska,[a] Karol Banaszak[a] and Paul Tordo[a]

Received 28th April 2006, Accepted 8th June 2006
First published as an Advance Article on the web 30th June 2006
DOI: 10.1039/b606062e

The free radical trapping properties of eight 5-alkoxycarbonyl-5-methyl-1-pyrroline *N*-oxide (EMPO) type nitrones and those of 5,5-dimethyl-1-pyrroline *N*-oxide (DMPO) were evaluated for trapping of superoxide anion radicals in the presence of 2,6-di-*O*-methyl-β-cyclodextrin (DM-β-CD). ^{1}H-NMR titrations were performed to determine both stoichiometries and binding constants for the diamagnetic nitrone–DM-β-CD equilibria. EPR titrations were then performed and analyzed using a two-dimensional EPR simulation program affording 1 : 1 and 1 : 2 stoichiometries for the nitroxide spin adducts with DM-β-CD and the associated binding constants after spin trapping. The nitroxide spin adducts associate more strongly with DM-β-CD than the nitrones. The ability of the nitrones to trap superoxide, the enhancement of the EPR signal intensity and the supramolecular protection by DM-β-CD against sodium L-ascorbate reduction were evaluated.

Introduction

Reactive oxygen species (ROS) have benefited from intense attention because of their implication in oxidative stress and a range of pathological processes.[1] Since the discovery of DMPO or PBN as spin traps, significant advances to find more efficient molecular systems trapping the ROS with enhanced lifetime of the resulting spin adducts have been realized with the synthesis of better nitrone spin traps.[2,3] Among recently reported nitrones, EMPO analogues (Fig. 1) are efficient spin traps for the detection of carbon and oxygen centered free radicals by electron paramagnetic resonance (EPR) spectroscopy.[3] Unfortunately, use of these traps for the detection of ROS in biological media is limited by the presence of species that reduce instantaneously the nitroxide spin adducts into EPR silent hydroxylamines.[4] To overcome these difficulties, cyclodextrins (CDs) are effective in (i) increasing the EPR signal intensity, (ii) lengthening the life time of superoxide spin adducts, and (iii) protecting the nitroxide spin adducts resulting from spin trapping against enzymatic or chemically reductive species.[5]

For paramagnetic guests, EPR was successfully used to study inclusion complexes of stable free radicals in cyclodextrins[6] for molecular[6c,7] and chiral[8] recognition and in terms of multimodal inclusion complexes.[6b,c,9] Bioreduction experiments were also performed with persistent nitroxides to test their ability to be protected against reduction by ascorbic acid[10] through inclusion in a cyclodextrin. However, the use of macrocycles during the detection

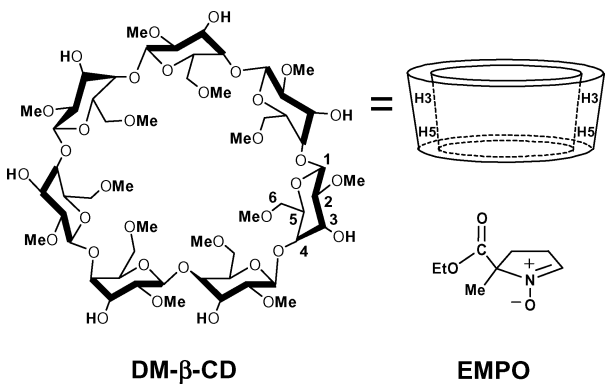

Fig. 1 Chemical structures of DM-β-CD and EMPO.

of transient free radicals by the spin trapping-EPR technique is quite recent. Chen and co-workers[11] have studied the trapping of carbon-centered radicals with nitroso compounds stabilized by cyclodextrins. However, cyclic nitrones are a better choice to trap superoxide as illustrated by 5-diethoxyphosphoryl-5-methyl-1-pyrroline *N*-oxide (DEPMPO) in the absence of cyclodextrin.[2a] Inclusion of PBN nitrones in β-cyclodextrin[12] and especially their methylated derivatives led to improved detection of superoxide radical *in vitro* and its observation under reductive conditions.[5c]

Moreover, the binding of PBN–superoxide spin adducts resulted in multiple equilibria due to the heteroditopic character of the PBN skeleton. This situation was analyzed in terms of microscopic binding constants and site interaction parameter (cooperativity).[5c,13] However, in spite of the recognized trapping properties of PBN, the oxygen free radicals derived spin adducts are less stable than those resulting from the trapping by EMPO analogues. In addition, with EMPO analogues, only 1 : 1 inclusion complexes are expected between the CDs and both the nitrones and the spin adducts. Therefore, we decided to investigate the

[a]*Laboratoire SREP, UMR 6517 CNRS et Universités d'Aix-Marseille 1, 2 et 3, Avenue Escadrille Normandie Niemen, Marseille, 13397, France. E-mail: jean-pierre.finet@up.univ-mrs.fr; Fax: + 33 491 288 758; Tel: + 33 491 288 927*
[b]*Chemical Research Center, Institute for Structural Chemistry, H-1525, Budapest, PO Box 17, Hungary*

† Electronic supplementary information (ESI) available: Synthesis yields, NMR spectra and additional figures. See DOI: 10.1039/b606062e

 This journal is © The Royal Society of Chemistry 2006

influence of DM-β-CD on the spin trapping of superoxide anion radical by a series of EMPO analogues.

Results and discussion

Synthesis

A range of EMPO ester derivatives was selected to cover a large scale of binding constants with DM-β-CD, considering that the more the nitrones are associated with the cyclodextrin, the less they can trap free radicals.[5c] Nitrones **2d** and **4d** to **9d** were prepared by an adaptation of the four step procedure of Zhao *et al.*[3c] (Scheme 1 and Electronic Supplementary Information, ESI†), whereas EMPO **3d** was prepared by the procedure of Olive *et al.*[3a]

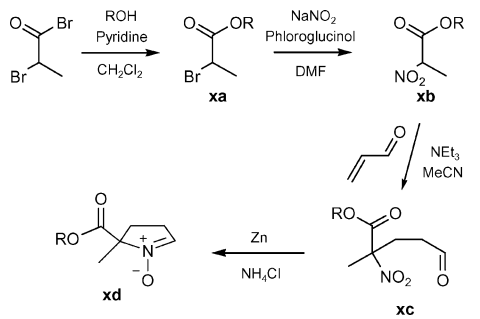

Scheme 1 General synthetic route to ester functionalized EMPO type nitrones (**x** refers to the alkoxy group, Fig. 2).

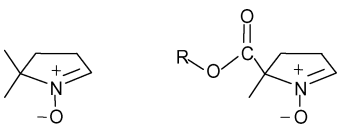

Nitrone	Number	R
DMPO	**1d**	-
MeMPO	**2d**	Methyl
EMPO	**3d**	Ethyl
*i*PrMPO	**4d**	*iso*- Propyl
*s*BuMPO	**5d**	*sec*-Butyl
BnMPO	**6d**	Benzyl
*t*BuMPO	**7d**	*tert*- Butyl
*n*PtMPO	**8d**	*neo*-Pentyl
CMMPO	**9d**	Cyclohexylmethyl

Fig. 2 Chemical structure of DMPO and of the synthesized EMPO and analogues.

NMR study

The characteristic features of the inclusion complexes between EMPO-type nitrones and 2,6-di-*O*-methyl-β-cyclodextrin were determined by ^{1}H-NMR studies. To study the effect of the host–guest association, the use of NMR spectroscopy was selected, as it provides specifically ^{1}H and ^{13}C complexation induced shifts (CIS) upon inclusion and represents a powerful tool to investigate molecular edifices in solution.[14] The ^{1}H-NMR signals of all the nitrones were first carefully assigned for D_2O solution of the nitrones alone (ESI†). All the signals related to the ester part of the nitrones were easily attributed except for *s*BuMPO **5d** and CMMPO **9d** for which 2D-NOESY spectra were necessary for a non ambiguous assignment. The methylene protons of the pyrroline ring exhibited three multiplet signals and were also assigned using 2D-NOESY in D_2O (ESI†).

Continuous variation method

The continuous variation method (Job's plot)[15] was used to determine the stoichiometry of the inclusion complexes. NMR samples were prepared by mixing equimolar amounts of freshly made stock solutions of β-CD and nitrone (10 mM) in different volumes leading to the desired values of the ratio $S_H = [H]_0/([H]_0 + [G]_0)$, with the total products concentration kept constant (V_{tot} = 500 μL) while the molar fractions of both components varied from 0 to 1 by steps of 0.1. The averaged values were monitored as a function of the cyclodextrin and nitrone concentrations. In preliminary experiments with D_2O solutions of the nitrones in the presence of DM-β-CD, significant ^{1}H-NMR complexation induced shifts (CIS) showed the presence of inclusion complexes. The mean values of the affected protons between the free and included guests suggested a fast exchange process between both species on the NMR timescale. However, the signal of the methyl group that substitutes the pyrroline ring was split into two signals during the titration whatever the nitrone. In spite of limited changes detectable in the ^{1}H-NMR spectra in the case of DMPO **1d**, MeMPO **2d** and EMPO **3d** in the presence of DM-β-CD, a 1 : 1 stoichiometry was derived from the Job's analysis of the CIS values for all the considered nitrones (see Fig. 3 for an example with CMMPO as a guest).

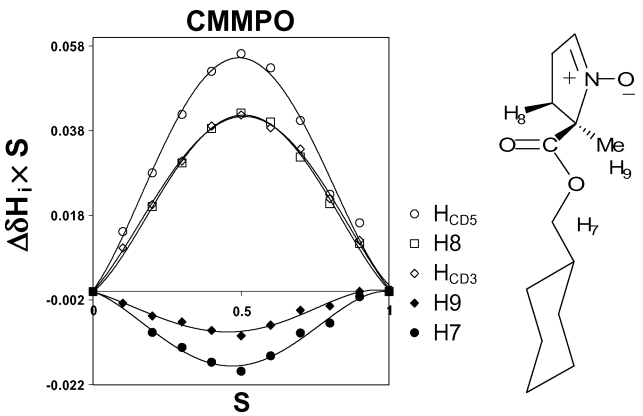

Fig. 3 Job's diagram for CMMPO **9d**–DM-β-CD equilibrium. (H_{CD3}, H_{CD5} = protons inside the DM-β-CD cavity, see Fig. 1).

Structure–complexation induced shift correlations

For each nitrone, the maximum CIS values were derived from the two extreme spectra (free of CD and maximum concentration of CD), affording information on the inclusion mode of the guests inside the CD cavity (Table 1). Nitrones **1d**, **2d** and **3d**, bearing poorly hydrophobic groups, showed only moderate CIS. Because of the good water solubility of these nitrones, they did not exhibit great affinity for the hydrophobic inner cavity of DM-β-CD. On the other hand, substitution of the ester function by bulkier alkyl groups resulted in a greater affinity for the CD cavity. Indeed, whereas the CIS of the nitronyl proton H7 decreased from nitrone

Table 1 ^{1}H NMR CIS values of EMPO analogues in the presence of DM-β-CD

Nitrone	Structure	H7	H8	H9	H10
1d	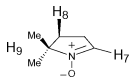	−0.03	+0.03	[a]	+0.04
2d	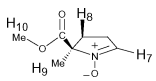	−0.05	−0.03	+0.04	[a]
3d	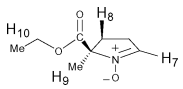	−0.05	−0.07	+0.04	+0.01
4d	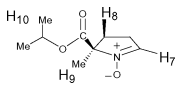	−0.04	−0.14	+0.03	+0.04
5d	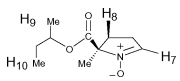	−0.03	−0.16	+0.08	+0.08
7d	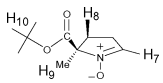	−0.05	+0.05	+0.01	+0.08
8d	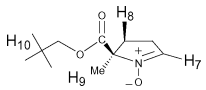	−0.02	−0.15	+0.05	+0.10
9d	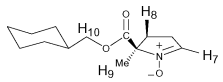	[a]	−0.10	+0.06	+0.10
6d	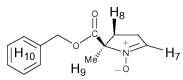	[a]	−0.32	+0.04	[a]

[a] $|\Delta\delta| < 0.01$ ppm.

2d to **9d** (except in the case of **7d**), the CIS observed on the alkyl ester region (H10) increased. Thus, the part of the nitrone that is included in the CD cavity seems to change, depending on the nature of the ester group. Replacement of the small methyl ester group by the bulkier *tert*-butyl or *neo*-pentyl group shifts the site, that is preferentially recognized by the CD, from the pyrroline ring to the ester moiety. In parallel, the general strength of the association is directly correlated with the nature of the ester group (see binding constants in Table 2). Although the fit between alkyl groups and the inside cavity of DM-β-CD should be better for the cyclohexyl group (and optimal for the adamantyl group, although not studied in the present series), the highest CIS were not observed in the case of nitrone **9d**. Moreover, the usually good affinity of the phenyl group for the inner β-CD cavity was not observed in the case of BnMPO **6d**. Instead of recording a significant CIS value for the aromatic protons (H10), a relatively big CIS was observed for the pyrroline proton H8. Besides, the absolute value for H8 CIS increased from +0.03 to +0.32 ppm on going from nitrone **1d** to nitrone **6d** (in the order displayed in Table 1 except for nitrones **7d** and **9d**). This trend is unusual since, in most cases, the H8 proton exhibits the highest CIS value compared to the other protons with the exclusion of other pyrroline ring protons. This might be related to a difference in the nitrone conformations implying that, during the titration, the C–H8 bond interacts with the asymmetric cone of the adjacent C=O bond.[16]

However, this hypothesis does not explain the CIS observed in the case of benzyl ester nitrone **6d**, since H8 is the only proton to give detectable and high CIS, while the rest of the molecule is not affected. X-Ray crystallographic analyses of the benzyl ester nitrone **6d** and of the corresponding saturated cyclohexylmethyl ester nitrone **9d** helped us to understand this behaviour (ESI†). BnMPO **6d** adopts a folded down (*cis*) conformation (ESI†) with the phenyl group slightly facing the nitrogen atom of the nitrone function. On the other hand, CMMPO **9d** exhibits an unfolded geometry (*trans*) with the cyclohexyl group opposite to the pyrroline ring (ESI†). The 5.6 Å distance between the positively charged nitrogen atom and the π cloud for BnMPO **6d** is too large to allow a stabilizing effect (angle between the 6-membered and the 5-membered ring planes of around 51°, ESI†). Nevertheless, the folded face-to-face geometry could be explained by a π–π and a pyrrolinyl CH–π interaction (around 2.8 and 2.7 Å respectively for each CH–π distance, see Fig. 4a and ESI†) that probably stabilizes each phenyl group.[17]

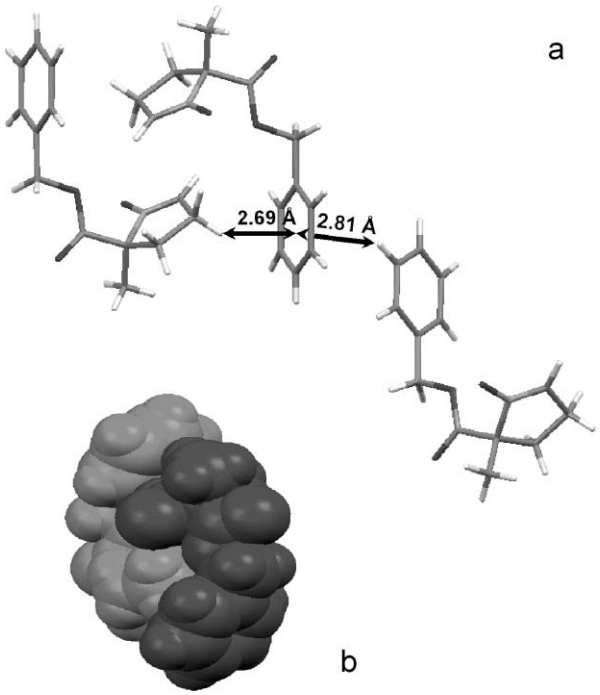

Fig. 4 Weak stabilizing interactions in the crystal structure of BnMPO **6d** and yin-yang-like disposition of two nitrone molecules.

The weak interactions (Fig. 4a) may be related to the observed relative disposition of two molecules of **6d** that is reminiscent of the yin-and-yang symbol (Fig. 4b). The folded conformation of BnMPO **6d** can prevent the phenyl group from being included in the CD cavity due to steric hindrance (this would explain the absence of CIS for aromatic protons H10). In contrast to the BnMPO nitrone **6d**, the CMMPO nitrone **9d** adopts an unfolded geometry allowing the cyclohexyl moiety to be complexed by the DM-β-CD. One hydrogen bond per molecule can be observed between the nitronyl proton of one molecule of **9d** and the carbonyl oxygen of a second one (≈2.4 Å distance, Fig. 5a). An almost

 This journal is © The Royal Society of Chemistry 2006

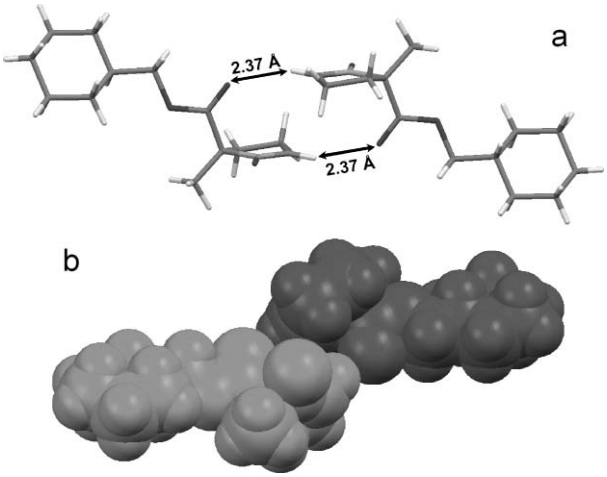

Fig. 5 Opposite disposition of the ester moieties in the crystal structure of CMMPO **9d** leading to a sheet-like structure in the solid state.

face-to-face disposition of the pyrroline rings is observed (Fig. 5b and ESI†) with the cyclohexyl moieties far apart. This alternation of hydrophobic cyclohexyl and hydrophilic nitrone packing zones leads to an overall sheet-like structure (see ESI†).

Thus, the solid state information may explain the absence of CIS for the aromatic protons of molecule **6d** due to the folded geometry of the nitrone, contrary to the unfolded one for nitrone **9d**. However, the effect of the solvent can play an important role on the nitrone geometry and, in spite of this structural information, the observed CIS for H8 of nitrone **6d** in solution with the exclusion of the other protons cannot be fully rationalized.

Calculation of association constants[16]

The ^{1}H-NMR titration technique was used to evaluate the binding constants. The whole sets of nitrone protons chemical shifts were monitored with the guest concentration kept constant, while the DM-β-CD concentration was increased (Fig. 6).

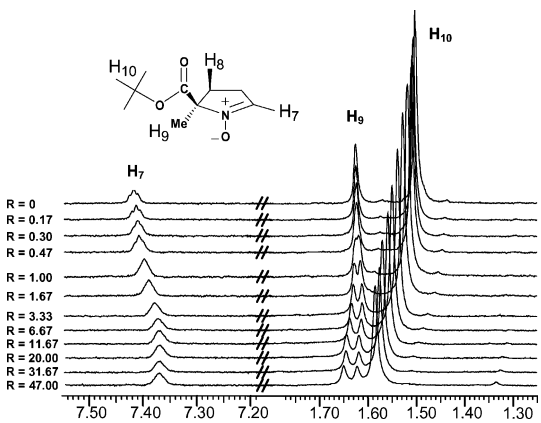

Fig. 6 Chemical shift evolution for selected guest protons during ^{1}H NMR titration of *t*BuMPO **7d** in the presence of DM-β-CD (R = [CD]/[nitrone]).

Formation of 1 : 1 complexes was assumed from the results of the continuous variation method. The Macomber model was then chosen to calculate the binding constants from the titration curves.[18] The non linear curve fitting procedure of these curves toward experimental points afforded the equilibrium constants (Fig. 7).

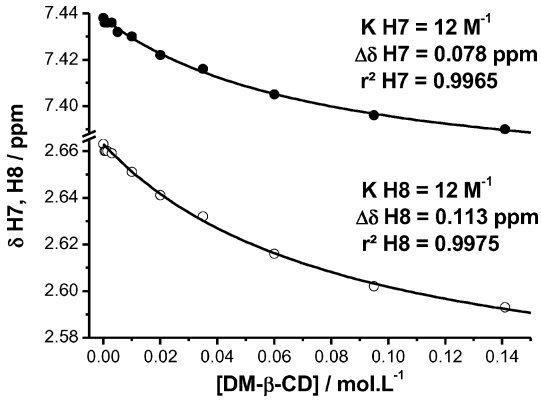

Fig. 7 Calculation of binding constants by non linear curve fitting of the chemical shift of the suitable EMPO **3d** protons investigated as a function of DM-β-CD concentration.

All protons affording convergent fit were considered. The weak intensity of the H8 signal made its detection rather tedious up to 35 mM of CD. Thus the CD concentration domain was limited in this case (Table 2). The useful range of CD concentrations has also been restricted for *n*PtMPO **8d** and CMMPO **9d** since a poor fit was obtained, if all points were considered.[8d] Correlation coefficients exceeded 0.99 except for a few cases. Calculations afforded estimations of maximum CIS and the value of binding constants related to the considered proton, with the errors estimated as previously described.[12] Finally, when more than one binding constant was estimated for a nitrone because of the different influence of the solvent on the nitrone protons in the complex, an averaged binding constant value was considered to give a more significant equilibrium constant with DM-β-CD.[19] The first aim was to detect a clear trend in the nitrone complexation by DM-β-CD. The results are reported in Table 2. The values of the binding constants were also used for the EPR titrations to estimate the binding constants between the spin adducts and DM-β-CD after superoxide trapping. In agreement with the CIS studies, the highly water soluble nitrones presented moderate binding constants (4 to 43 M^{-1} from MeMPO **2d** to *s*BuMPO **5d**), with only slight differences upon the considered protons. In the case of bulky ester groups (like *tert*-butyl), the binding constants exceeded 200 M^{-1}. The independent values are homogeneous for CMMPO **9d**, close to 960 M^{-1} but more dispersed for *t*BuMPO **7d** and *n*PtMPO **8d**. Nevertheless, a clear trend can be observed in the series with binding constant values increasing regularly with the size of the ester group from 4 M^{-1} for the smallest (MeMPO **2d**) to 962 M^{-1} for the bulkiest (CMMPO **9d**). These calculated maximum CIS and binding constant values agree well with the previous analysis of experimental CIS and with the continuous variation method. On the other hand, it must be remembered that the values estimated from equilibria occurring in deuterated water are probably slightly overestimated compared to the experiments in water.[20] So, nitrones **1d** to **7d** showed moderate binding constants toward DM-β-CD in line with good trapping properties (sufficient availability of the trap toward free radicals). On the contrary, *n*PtMPO **8d** and CMMPO **9d** were expected to

Table 2 Binding constants and maximum ^{1}H-NMR CIS for the different nitrones based on the selected protons, toward DM-β-CD

Entry	Nitrone	Proton	K_{Hi}/M^{-1}	$\|\Delta\delta\|$ (ppm)	r^2	[CD]/mM	K_{NMR}/M^{-1}
DMPO	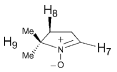	H7	24 (±4)	0.035 (±0.003)	>0.994	0.5–141	24
MeMPO	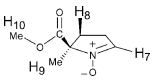	H7 H8	4 (±1) 3 (±1)	0.128 (±0.019) 0.102 (±0.019)	>0.988 >0.972	0.5–141 0.5–141	4
EMPO	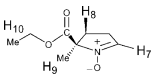	H7 H8	12 (±3) 12 (±2)	0.078 (±0.009) 0.113 (±0.012)	>0.996 >0.997	0.5–141 0.5–141	12
*i*PrMPO	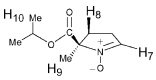	H7 H8	32 (±6) 22 (±2)	0.052 (±0.004) 0.218 (±0.011)	>0.991 >0.998	0.5–141 0.5–95	27
*s*BuMPO	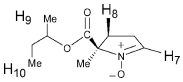	H8 H9 H10	78 (±7) 22 (±4) 28 (±5)	0.213 (±0.008) 0.104 (±0.006) 0.103 (±0.008)	>0.991 >0.992 >0.992	0.5–35 0.5–141 0.5–141	43
BnMPO	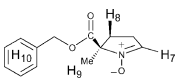	H8	207 (±13)	0.343 (±0.007)	>0.998	0.5–95	207
*t*BuMPO	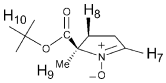	H7 H10	379 (±51) 80 (±8)	0.051 (±0.002) 0.085 (±0.002)	>0.987 >0.982	0.5–141 0.5–141	230
*n*PtMPO	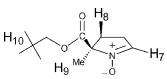	H8 H9 H10	678 (±156) 294 (±50) 314 (±29)	0.157 (±0.008) 0.033 (±0.002) 0.074 (±0.002)	>0.992 >0.982 >0.995	0.5–35 0.5–35 0.5–35	429
CMMPO	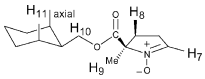	H9 H10 H11	843 (±130) 1052 (±104) 990 (±103)	0.039 (±0.001) 0.092 (±0.002) 0.093 (±0.002)	>0.988 >0.997 >0.995	0.5–35 0.5–35 0.5–35	962

trap less efficiently the superoxide in the presence of DM-β-CD due to their higher affinity toward the CD cavity.

EPR study

Preliminary EPR spectra of the spin adducts of superoxide trapped by nitrones **1d–9d** in the presence of DM-β-CD were recorded under identical experimental conditions. In a previous study,[5c] we found that decreasing intensity of the EPR spectrum is associated with increasing binding constants of the corresponding nitrone–CD couples. In the present series of nitrones, EMPO **3d**, *s*BuMPO **5d** and BnMPO **6d** showed the highest EPR spectrum intensity. However, in the case of the two bulkiest nitrones (*n*PtMPO **8d** and CMMPO **9d**) the spin trapping reaction is impeded (nitrones exhibiting the larger binding constants with cyclodextrins) compared to the smaller nitrones **1d–7d**. The high signal intensity in the case of nitrones **3d**, **5d** and **6d** can be assigned to the known good stability of the superoxide spin adducts, allowing a more efficient accumulation of the paramagnetic species compared to the case of other nitrones. Thus, the affinity of the trap for the cyclodextrin is important to predict the trapping efficiency; but the intrinsic stability of the superoxide spin adduct plays also an important role for free radical detection. The EPR signal enhancement can be attributed to inclusion of the nitroxide spin adduct in the CD unless the parent nitrone is too strongly complexed by the CD to allow good trapping.

Calculations of association constants

In the EPR titration experiments, the global amount of cyclodextrin is expected to be shared between all products susceptible to be complexed: the nitrones and their superoxide adducts (Fig. 8). The nitrone concentration being much larger than that of the nitroxides, the proportion of CD occupied for complexation of the nitrones is crucial for estimation of the free CD, which can be estimated by K_{NMR}.

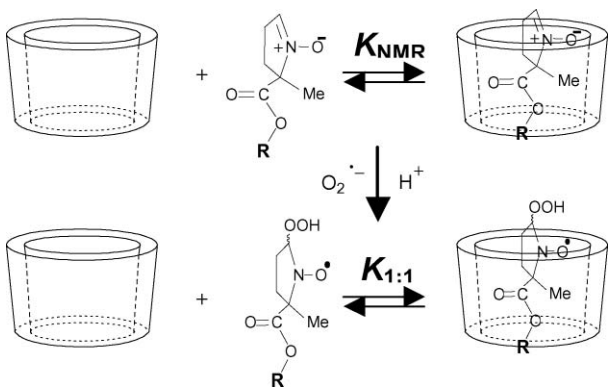

Fig. 8 Schematic representation of equilibria occurring before and after spin trapping of superoxide by EMPO analogues in the presence of DM-β-CD.

This journal is © The Royal Society of Chemistry 2006

As previously reported in the case of PBN derivatives used as spin traps,[5c] the EPR spectra intensities are also correlated to the added CD concentration (Fig. 9). The pattern of the EPR spectra shows continuous variation in the titrations presenting the superimposition of free and included species. The association properties of pyrroline type nitrone spin adducts differ from those of the open chain nitrones: for the ring compound, only two types of association can be observed contrary to the PBN derivatives, where two different single and one double association can be formed. In the EMPO type series, efforts to distinguish the free and complexed species of the *cis* and *trans* superoxide spin adducts by 2D-EPR simulations[21] were not successful due to the poor resolution. Although the fit become better, the large number of adjusted parameters made the confidence of the spectral decomposition rather poor. A further difficulty is the presence of a chemical exchange phenomenon[3a] that is also a source of error, which can prevent the most sophisticated analysis. For these reasons, we considered only a simpler rigid superimposed model concerning the 1 : 1 association.

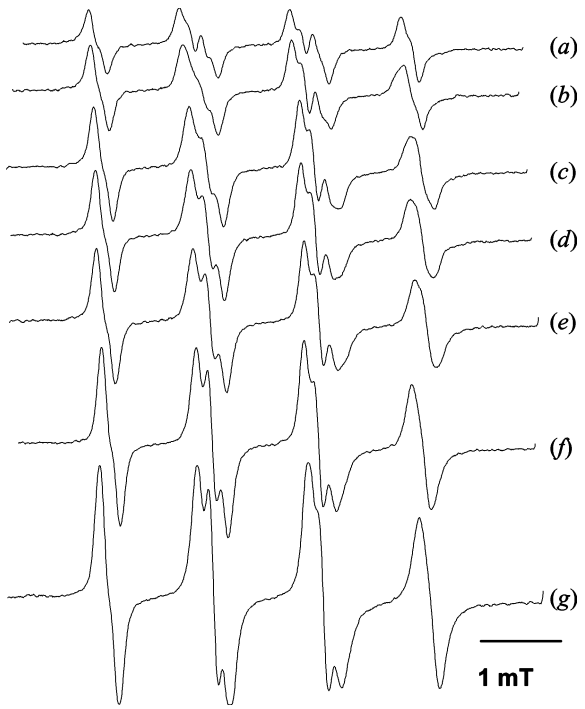

Fig. 9 Selected EPR spectra of EMPO **3d** superoxide spin adduct with increasing concentration of DM-β-CD: superoxide spin adduct (*a*) without CD, (*b*) with CD 3 mM, (*c*) 6 mM, (*d*) 9 mM, (*e*) 12 mM, (*f*) 25 mM, (*g*) 100 mM.

In spite of these limitations, 2D-EPR simulations implying free (1 : 0), single associated (1 : 1) and double associated (1 : 2) nitroxides gave the best results. Thus, the possibility of encapsulation followed by dimerization of DM-β-CD at high CD concentrations was once again observed.

The results of 2D spectral decompositions of the EPR titrations are reported in Table 3.

A convincing proof of spin adduct encapsulation in the CD cavity is given by the decrease of the nitrogen splitting constant a_N that reflects the lower polarity of the environment in the vicinity of the nitroxide function, which is the case of inner cavity of the CD. Further evidence for the association is given by the high field lines of the spectrum that have smaller amplitude than the other lines in the cases of 1 : 1 and 1 : 2 species, a clear indication of the restriction of the molecular rotation upon inclusion (see Fig. 9).

Table 3 Calculated values of binding constants and EPR parameters for spin trapping of superoxide in the presence of DM-β-CD

Nitrone	Param.[a]	1 : 0[b]	1 : 1[c]	1 : 2[d]	K_{NMR}[e]	a[f]
DMPO	a_N/mT	1.413	1.343	1.334	24	14.3
	a_H/mT	1.137	1.104	1.048		
	$a_{H'}$/mT	0.118	0.121	0.177		
	K/M^{-1}		343	603		
MeMPO	a_N/mT	1.306	1.250	1.248	4	28.3
	a_H/mT	1.084	1.102	1.003		
	$a_{H'}$/mT	0.101	0.106	0.124		
	K/M^{-1}		113	129		
EMPO	a_N/mT	1.317	1.247	1.248	12	17.3
	a_H/mT	1.086	1.103	0.999		
	$a_{H'}$/mT	0.103	0.107	0.132		
	K/M^{-1}		207	307		
*i*PrMPO	a_N/mT	1.320	1.249	1.253	27	9.9
	a_H/mT	1.096	1.090	1.082		
	$a_{H'}$/mT	0.102	0.114	0.102		
	K/M^{-1}		266	2 985		
*s*BuMPO	a_N/mT	1.321	1.249	1.259	43	8.5
	a_H/mT	1.085	1.078	1.072		
	$a_{H'}$/mT	0.104	0.118	0.100		
	K/M^{-1}		367	3 510		
BnMPO	a_N/mT	1.317	1.250	1.251	207	3.1
	a_H/mT	1.077	1.063	1.082		
	$a_{H'}$/mT	0.101	0.119	0.075		
	K/M^{-1}		645	7 340		
*t*BuMPO	a_N/mT	1.333	1.267	1.271	230	2.9
	a_H/mT	1.097	1.088	1.080		
	$a_{H'}$/mT	0.106	0.113	0.110		
	K/M^{-1}		658	18 500		
*n*PtMPO	a_N/mT	1.317	1.265	1.268	429	2.1
	a_H/mT	1.074	1.039	1.090		
	$a_{H'}$/mT	0.105	0.124	0.061		
	K/M^{-1}		892	3 950		
CMMPO	a_N/mT	1.326	1.278	1.243	962	2.2
	a_H/mT	1.086	1.048	1.094		
	$a_{H'}$/mT	0.106	0.118	0.105		
	K/M^{-1}		2 144	133700		

[a] EPR spectra parameters. [b] Parameters for the free nitroxides. [c] Parameters for the 1 : 1 complexes. [d] Parameters for the 1 : 2 complexes. [e] In M^{-1}. [f] $a = K_{1:1}/K_{NMR}$

The possibility for the 2D EPR simulation program to take into account the previously calculated K_{NMR} greatly helped for a reliable determination of nitroxide–CD binding constants. As for PBN, the 1 : 1 nitroxide binding constants are found always larger for the included spin adducts than for the parent nitrones toward DM-β-CD complexation (Fig. 10).[5c]

The trend in the values of $K_{1:1}$ for the nitroxide–CD pair is the same as for K_{NMR} considering the changes in the ester function. Indeed, a clear increase of $K_{1:1}$ with bulkier nitroxide ester parts can be seen. On the other hand, the a ratio ($K_{1:1}/K_{NMR}$) also named selectivity is decreasing with the general size of the spin adducts depending on the nitrone considered.

This trend can be explained by the differences in size and polarity for each nitrone and corresponding nitroxide considered. Indeed, the effect on complexation when the superoxide spin adduct is formed is more intense for the smaller nitrones than for the bigger nitrones. On the other hand, the larger calculated $K_{1:2}$ binding constants compared to $K_{1:1}$ support the occurrence of

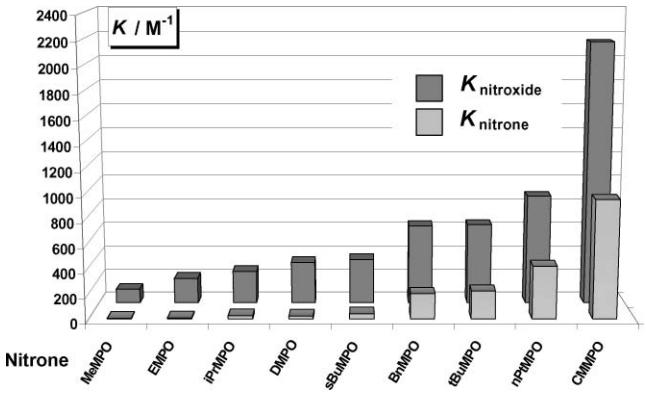

Fig. 10 Comparison of (spin adduct) nitroxide–CD binding constants (dark grey) and nitrone–CD binding constants (light grey) for all the considered nitrones.

DM-β-CD dimerization with the superoxide adducts as included guest at high CD concentration. Nevertheless, calculation of the stepwise binding constants according to Connors[13] shows a non cooperative complexation process.

This is probably due to the difference in polar surfaces of the superoxide spin adducts (ester hydrophobic part *versus* more hydrophilic hydroperoxy-nitroxide group). Complexation of the ester function can be expected easier than complexation of the hydroperoxy-nitroxide counterpart.

Bioreducing experiments

Despite the efficient spin trapping properties of EMPO, its derivatives were only seldom applied as traps in biological media since the resulting spin adducts are instantaneously reduced. It is promising, however, that the cyclodextrins proved effective in protecting the superoxide spin adducts against enzymatic and molecular reduction in the case of DEPMPO[5a] and PBN derivatives as spin traps.[5b,5c] In the case of the superoxide adducts of EMPO analogues **1d–9d** under reductive conditions, the EPR spectrum of EMPO superoxide spin adduct can be recorded up to 3 minutes in the presence of DM-β-CD (Fig. 11).

The other EMPO analogue nitrones as spin traps did not exhibit a higher observed time except in the case of *s*BuMPO **5d** (up to 4 minutes: see Table 4).

Moreover significant differences in the decrease of the EPR signal intensity (linked to the nitroxide concentration) were monitored after the first minute of reduction (data not shown). However, this trend cannot be correlated to the maximum time of observation of the nitroxides since it is affected both by the ability to trap the superoxide and by the stability of the resulting spin adducts. The nitroxide spin adducts derived from EMPO **3d** and *s*BuMPO **5d** exhibited the longest observation time of the signal, and these nitrones produced also the greatest EPR spectrum intensity all things being otherwise equal. That would explain that, in spite of a rapid loss of signal for EMPO-OOH EPR spectrum, the signal observation time is still rather long. Finally, we did not observe any direct correlation between the estimated nitroxide binding constants toward DM-β-CD and the resistance abilities of these complexed spin adducts toward L-ascorbate. However, the presence of DM-β-CD undoubtedly slows down the reductive process.

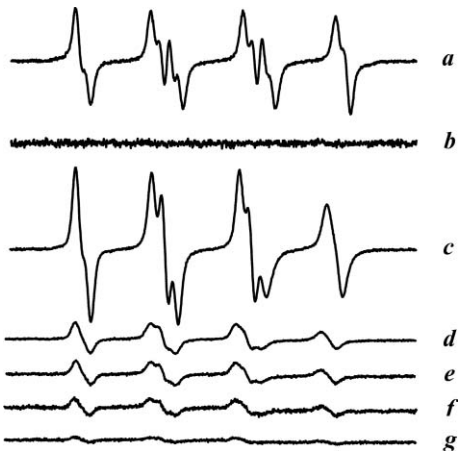

Fig. 11 Protection of the EMPO-OOH nitroxide spin adduct by DM-β-CD (50 mM) against sodium L-ascorbate reduction. (*a*) EMPO-OOH EPR signal in the absence of cyclodextrin. (*b*) Signal obtained after addition of SOD and sodium L-ascorbate (*c*) EMPO-OOH EPR signal in the presence of DM-β-CD. (*d*) 1 min 15 s after addition of SOD and sodium L-ascorbate (0.1 mM). (*e*) After 2 min. (*f*) After 2 min 45 s. (*g*) After 3 min 30 s.

Table 4 Maximum time of EPR observation of the superoxide spin adducts under reductive conditions (0.1 mM sodium L-ascorbate)

Entry	Nitrone	t_{obs}
1d	DMPO	3 min
2d	MeMPO	2 min 50 s
3d	EMPO	3 min 30 s
4d	*i*PrMPO	2 min 20 s
5d	*s*BuMPO	4 min 10 s
6d	BnMPO	1 min 40 s
7d	*t*BuMPO	1 min
8d	*n*PtMPO	1 min 40 s
9d	CMMPO	2 min 20 s

Conclusion

EMPO type nitrones are significantly complexed by 2,6-di-*O*-methyl-β-cyclodextrin (DM-β-CD) and the complexation strongly depends on the nature of the ester function. Trapping of superoxide radical by these nitrones does not hinder the complexation process by the DM-β-CD. The strength of the spin adduct recognition even increases by formation of the less polar nitroxide group that replaces the strongly polar nitrone structure after spin trapping. The stabilization induced by complexation affords a better detection due to the enhanced EPR spectrum intensities, unless the too strongly complexed nitrones block the trapping process. Contrary to PBN, the difference in polarity for the heteroditopic EMPO superoxide spin adduct (ester side and hydroperoxy-nitroxide group) induces a non-cooperative situation. Indeed, at high DM-β-CD concentration a second complexation effectively occurs, but less efficient than the first one. Nevertheless, DM-β-CD dimerizes to encapsulate the unstable superoxide spin adducts. Thus, cyclodextrins should promote the use of nitrone type spin traps for the direct observation and the characterization of free radicals, in particular, the ROS species in *ex vivo* or *in vivo* EPR experiments.

This journal is © The Royal Society of Chemistry 2006

Experimental

General

All commercially available chemicals and organic solvents were used as received without further purification. 2,6-Di-*O*-methyl-β-cyclodextrin was purchased from Acros Organics. Xanthine oxidase (XOD) and diethylenetriaminepentaacetic acid (DTPA) were from Sigma Chemical Co. Crude materials were purified by flash chromatography on Merck silica gel 60 (0.040–0.063 mm). ^{1}H-NMR and ^{13}C-NMR spectra were recorded with a Bruker DPX 300 spectrometer at 300.13 MHz and 75.54 MHz respectively. Chemical shifts (δ) are reported in ppm for a solution of the nitrone in $CDCl_3$ with internal reference Me_4Si (Euriso-Top, CEA Saclay, 99.80%). *J* values are reported in Hz. The assignments of NMR signals were facilitated by the use of DEPT135 and NOESY sequence in D_2O if necessary. Melting points were measured on a Büchi B-540 apparatus and are uncorrected.

The nitrones were prepared by the procedure described by Zhao *et al.*[3c] and only the characteristic physical data of the new compounds are reported.

5-Methoxycarbonyl-5-methyl-1-pyrroline *N*-oxide **2d**,[3g] 5-ethoxycarbonyl-5-methyl-1-pyrroline *N*-oxide **3d**,[3a] 5-(1-methylethoxy)carbonyl-5-methyl-1-pyrroline *N*-oxide **4d**,[3f] 5-(2-butoxycarbonyl)-5-methyl-1-pyrroline *N*-oxide **5d**[3f] and 5-(1,1-dimethylethoxycarbonyl)-5-methyl-1-pyrroline *N*-oxide **7d**[3c] were prepared by literature procedures.

Benzyl 1-oxo-4-nitro-4-methylpentanoate 6c. 95%, δ_H 1.79 (s, 3H), 2.46–2.59 (m, 4H), 5.23 (s, 2H), 7.31–7.40 (m, 5H), 9.70 (s, 1H).

5-Benzyloxycarbonyl-5-methyl-1-pyrroline *N*-oxide 6d. Flash chromatography (CH_2Cl_2–EtOH 95, 18.5 : 1.5), 10%, colourless crystals, mp 62 °C; δ_H 1.75 (s, 3H), 2.10–2.20 (m, 1H), 2.52–2.80 (m, 3H), 5.18 (d, *J* 12.4, 1H), 5.28 (d, *J* 12.3, 1H), 6.96 (t, *J* 2.6, 1H), 7.32–7.40 (m, 5H); δ_C 20.94, 25.84, 32.34, 67.69, 79.08, 127.98, 128.42, 128.61, 134.82, 135.12, 169.69. Calcd for $C_{13}H_{15}NO_3$, 0.1 CH_2Cl_2 (233.27 g mol^{-1}) C, 65.08; H, 6.34; N, 5.79. Found C, 65.27; H, 6.58; N, 5.69%.

2,2-Dimethylpropyl 2-bromopropanoate 8a. 97%, δ_H 0.97 (s, 9H), 1.84 (d, *J* 6.9, 3H), 3.82 (d, *J* 10.5, 1H), 3.92 (d, *J* 10.6, 1H), 4.41 (q, *J* 7.0, 1H).

2,2-Dimethylpropyl 2-nitropropanoate 8b. Flash chromatography (pentane–CH_3OH, 19.5 : 0.5), 38%, δ_H 0.94 (s, 9H), 1.82 (d, *J* 7.2, 3H), 3.89 (d, *J* 10.4, 1H), 3.95 (d, *J* 10.4, 1H), 5.25 (q, *J* 7.2, 1H).

2,2-Dimethylpropyl 1-oxo-4-nitro-4-methylpentanoate 8c. 92%, δ_H 0.94 (s, 9H), 1.81 (s, 3H), 2.44–2.66 (m, 4H), 3.90 (s, 2H), 9.78 (s, 1H).

5-(2,2-Dimethylpropoxycarbonyl)-5-methyl-1-pyrroline *N*-oxide 8d. Flash chromatography (CH_2Cl_2–CH_3OH, 18.5 : 1.5), 42%, white solid, mp 50–51 °C; δ_H 0.96 (s, 9H), 1.74 (s, 3H), 2.13–2.23 (m, 1H), 2.57–2.86 (m, 3H), 3.90 (d, *J* 10.5, 2H), 6.97 (t, *J* 2.6, 1H); δ_C 20.97, 25.83, 26.32, 31.54, 32.51, 75.13, 79.05, 134.36, 169.83. Calcd for $C_{11}H_{19}NO_3$, 0.1 H_2O (213.28 g mol^{-1}) C, 61.43; H, 9.00; N, 6.51. Found C, 61.53; H, 8.96; N, 6.48%.

Cyclohexylmethyl 2-bromopropanoate 9a. 66%, δ_H 0.92–1.05 (m, 2H), 1.14–1.33 (m, 3H), 1.67–1.77 (m, 6H), 1.83 (d, *J* 7.0, 3H), 3.92–4.04 (m, 2H), 4.37 (q, *J* 6.9, 1H).

Cyclohexylmethyl 2-nitropropanoate 9b. Flash chromatography (pentane–CH_3OH, 18 : 2), 60%, δ_H 0.9–1.02 (m, 2H), 1.13–1.32 (m, 3H), 1.64–1.77 (m, 6H), 1.80 (d, *J* 7.0, 3H), 3.90–4.04 (m, 2H), 5.22 (q, *J* 7.1, 1H).

Cyclohexylmethyl 1-oxo-4-nitro-4-methylpentanoate 9c. 97%, δ_H 0.89–1.01 (m, 2H), 1.13–1.31 (m, 3H), 1.61–1.75 (m, 6H), 1.80 (s, 3H), 2.42–2.65 (m, 4H), 4.02 (d, *J* 6.0, 2H), 9.77 (s, 1H).

5-Cyclohexylmethoxycarbonyl-5-methyl-1-pyrroline *N*-oxide 9d. Flash chromatography (pentane–AcOEt–CH_3OH, 12 : 5 : 3), 9%, colourless crystals, mp 52 °C; δ_H 0.91–1.03 (m, 2H), 1.13–1.31 (m, 3H), 1.62–1.73 (m, 6H), 1.73 (s, 3H), 2.12–2.22 (m, 1H), 2.55–2.85 (m, 3H), 4.01 (m, 2H), 6.97 (t, *J* 2.6, 1H); δ_C 20.97, 25.55, 25.85, 26.24, 29.50, 32.55, 36.95, 71.17, 79.05, 134.59, 169.93. Calcd for $C_{13}H_{21}NO_3$, 0.2 H_2O (239.31 g mol^{-1}) C, 64.28; H, 8.88; N, 5.77. Found C, 64.28; H, 8.81; N, 5.70%.

NMR measurements

All spectra were recorded at 300 K in D_2O (Euriso-Top, CEA Saclay, 99.90%), the residual HOD signal (δ 4.79 ppm) being used as the internal reference.[14]

Continuous variation method (Job's plot)

This technique was used as described previously for similar nitrone–cyclodextrin equilibria (10 mM final concentration).[5c]

Binding constant calculations

The results obtained in a precedent work for PBN analogue–cyclodextrin titrations helped in choosing the final nitrone concentration (3 mM) as well as the work range of DM-β-CD concentration (from 0.5 to 141 mM). The NMR experiments were performed as described previously.[5c] CIS values were determined by comparison of ^{1}H-NMR spectra of the nitrone alone and the mixture containing the nitrone and the maximum DM-β-CD concentration.

EPR measurements

EPR spectra were recorded at room temperature using a Bruker ESP 300 EPR spectrometer at 9.5 GHz (X-band) employing 100 kHz field modulation. All the solutions were prepared in a chelex-treated phosphate buffer (0.1 M, pH 7.4).

Superoxide trapping

The EMPO analogue (25 mM), diethylenetriaminepentaacetic acid (DTPA 0.5 mM) and hypoxanthine (HX 0.2 mM) were mixed in the presence of desired concentrations of DM-β-CD. To this oxygenated solution (bubbled during 1.5 min), xanthine oxidase (XOD 0.05 U mL^{-1}) was added to generate superoxide.

Binding constant calculations

EPR spectra were recorded at a fixed time after generation of superoxide (within five minutes) and a constant nitrone concentration (25 mM) was used. The amount of cyclodextrin was progressively increased (from 3 to 170 mM) to detect changes in

the spectral pattern of the EPR signal characteristic of superimposition between the free and included superoxide spin adducts. Deconvolution of EPR spectra from EPR titrations using the two-dimensional simulation software[21] afforded stoichiometries and binding constants of the nitroxide spin adducts toward DM-β-CD.

Sodium L-ascorbate reduction

Reaction mixture of EMPO analogues (25 mM) with DTPA (0.5 mM), HX (0.2 mM) and DM-β-CD (50 mM) were prepared followed by addition of XOD (0.05 U mL^{-1}) to start the trapping reaction. When the maximum of EPR signal intensity was reached (around 16 minutes), superoxide dismutase (SOD 50 U mL^{-1}) was added to the solution to stop the trapping of superoxide followed by subsequent addition of sodium L-ascorbate solution (0.1 mM final concentration).

X-Ray crystal structure determinations

Colourless prism type single crystals of compounds **6d** and **9d** suitable for X-Ray diffraction were obtained by slow evaporation of their solution in a pentane–Et_2O mixture within two days.

Crystal data for BnMPO 6d. $C_{13}H_{15}NO_3$, $M = 233.26$, monoclinic, $a = 10.2450(2)$, $b = 5.5640(10)$, $c = 21.3930(6)$ Å, $\beta = 102.24(8)°$, $U = 1191.75(5)$ Å^3, $T = 293(2)$ K, space group $P21/c$, $Z = 4$, μ(Mo-Kα) = 0.093 mm^{-1}, 3901 reflections measured, 3514 unique, $R_{int} = 0.036$, final $R = 0.058$.‡

Crystal data for CMMPO 9d. $C_{13}H_{21}NO_3$, $M = 239.31$, orthorhombic, $a = 9.5780(10)$, $b = 7.9730(10)$, $c = 35.1840(6)$ Å, $\beta = 90.00°$, $U = 2686.84(6)$ Å^3, $T = 293(2)$ K, space group $Pbca$, $Z = 8$, μ(Mo-Kα) = 0.083 mm^{-1}, 3360 reflections measured, 2912 unique, $R_{int} = 0.061$, final $R = 0.0541$.‡

Acknowledgements

The financial support of the Hungarian Scientific Research Fund through grants OTKA T-046953 and NKFP 1/A/005/2004 "MediChem2" is gratefully acknowledged. The authors thank the Conseil Régional Provence Alpes Côte d'Azur and TROPHOS Company for financial support. The Socrates program is also acknowledged for partial financial support of K. Banaszak and I. Biskupska. Sandrine Lambert, Dr Michel Giorgi, Dr Sylvain Marque and Dr Robert Faure are thanked for various contributions. DMPO was generously provided by Radical Vision (Marseille).

References

1 M. J. Davies and G. S. Timmins, *Electron Paramagn. Reson.*, 2000, **17**, 1–42.
2 (*a*) C. Fréjaville, H. Karoui, F. Le Moigne, M. Culcasi, S. Piétri, R. Lauricella, B. Tuccio and P. Tordo, *J. Chem. Soc., Chem. Commun.*, 1994, 1793–1794; (*b*) F. Chalier and P. Tordo, *J. Chem. Soc., Perkin Trans. 2*, 2002, 2110–2117; (*c*) A. Allouch, V. Roubaud, R. Lauricella, J. C. Bouteiller and B. Tuccio, *Org. Biomol. Chem.*, 2003, **1**, 593–598.
3 (*a*) G. Olive, A. Mercier, F. Le Moigne, A. Rockenbauer and P. Tordo, *Free Radical Biol. Med.*, 2000, **28**, 403–408; (*b*) H. Zhang, J. Joseph, J. Vasquez-Vivar, H. Karoui, C. Nsanzumuhire, P. Martásek, P. Tordo and B. Kalyanaraman, *FEBS Lett.*, 2000, **473**, 58–62; (*c*) H. Zhao, J. Joseph, H. Zhang, H. Karoui and B. Kalyanaraman, *Free Radical Biol. Med.*, 2001, **31**, 599–606; (*d*) K. Stolze, N. Udilova and H. Nohl, *Biol. Chem.*, 2002, **383**, 813–820; (*e*) F. A. Villamena and J. L. Zweier, *J. Chem. Soc., Perkin Trans. 2*, 2002, 1340–1344; (*f*) K. Stolze, N. Udilova, T. Rosenau, A. Hofinger and H. Nohl, *Biol. Chem.*, 2003, **384**, 493–500; (*g*) P. Tsai, K. Ichikawa, C. Mailer, S. Pou, H. J. Halpern, B. H. Robinson, R. Nielsen and G. M. Rosen, *J. Org. Chem.*, 2003, **68**, 7811–7817; (*h*) H. Karoui, J.-L. Clément, A. Rockenbauer, D. Siri and P. Tordo, *Tetrahedron Lett.*, 2004, **45**, 149–152; (*i*) K. Stolze, N. Udilova, T. Rosenau, A. Hofinger and H. Nohl, *Biochem. Pharmacol.*, 2005, **69**, 297–305.
4 (*a*) W. R. Couet, R. C. Brasch, C. Sosnovsky, J. Lukszo, I. Prakash, C. T. Gnewech and T. N. Tozer, *Tetrahedron*, 1985, **41**, 1165–1172; (*b*) R. J. Mehlhorn, *J. Biol. Chem.*, 1991, **266**, 2724–2731; (*c*) N. Kocherginsky and H. M. Swartz, *Nitroxide Spin Labels: Reactions in Biology and Chemistry*, CRC Press, Boca Raton, 1995, pp. 32–48; (*d*) E. J. Rauckman, G. M. Rosen and L. K. Griffeth, *Spin Labeling in Pharmacology*, ed. J. L. Holtzman, Academic Press, London, 1984, pp. 175–190; (*e*) M. Semjurc, S. Pecar, K. Chen, M. Wu and H. M. Swartz, *Biochim. Biophys. Acta*, 1991, **1073**, 329–335; (*f*) H. Hu, G. Sosnovsky, S. W. Li, N. U. M. Rao, P. D. Morse and H. M. Swartz, *Biochim. Biophys. Acta*, 1989, **1014**, 211–218.
5 (*a*) H. Karoui, A. Rockenbauer, S. Pietri and P. Tordo, *Chem. Commun.*, 2002, 3030–3031; (*b*) H. Karoui and P. Tordo, *Tetrahedron Lett.*, 2004, **45**, 1043–1045; (*c*) D. Bardelang, A. Rockenbauer, H. Karoui, J.-P. Finet and P. Tordo, *J. Phys. Chem. B*, 2005, **109**, 10521–10530.
6 (*a*) J. Martinie, J. Michon and A. Rassat, *J. Am. Chem. Soc.*, 1975, **97**, 1818–1823; (*b*) M. Lucarini, B. Luppi, G. F. Pedulli and B. P. Roberts, *Chem.–Eur. J.*, 1999, **5**, 2048–2054 and references therein; (*c*) Y. Kotake and E. G. Janzen, *J. Am. Chem. Soc.*, 1989, **111**, 5138–5140; (*d*) Y. Kotake and E. G. Janzen, *J. Am. Chem. Soc.*, 1992, **114**, 2872–2874 and references therein.
7 Y. Kotake and E. G. Janzen, *Free Radical Res. Commun.*, 1990, **10**, 103–108.
8 (*a*) J. Michon and A. Rassat, *J. Am. Chem. Soc.*, 1979, **101**, 995–996; (*b*) J. Michon and A. Rassat, *J. Am. Chem. Soc.*, 1979, **101**, 4337–4339; (*c*) E. G. Janzen and Y. Kotake, *J. Am. Chem. Soc.*, 1988, **110**, 7912–7913; (*d*) P. Franchi, M. Lucarini, E. Mezzina and G. F. Pedulli, *J. Am. Chem. Soc.*, 2004, **126**, 4343–4354.
9 Y. Sueishi, M. Kasahara and Y. Kotake, *Chem. Lett.*, 2000, 792–793.
10 (*a*) C. Ebel, K. U. Ingold, J. Michon and A. Rassat, *Nouv. J. Chim.*, 1985, **9**, 479–485; (*b*) C. Ebel, K. U. Ingold, J. Michon and A. Rassat, *Tetrahedron Lett.*, 1985, **26**, 741–744; (*c*) M. Okazaki and K. Kuwata, *J. Phys. Chem.*, 1985, **89**, 4437–4440.
11 (*a*) L. B. Luo, D.-Y. Han, Y. Wu, X. Y. Song and H.-L. Chen, *J. Chem. Soc., Perkin Trans. 2*, 1998, 1709–1714; (*b*) Y. Chen, H.-L. Chen, Q.-C. Yang, X.-Y. Song, C.-Y. Duan and T. C. W. Mak, *J. Chem. Soc., Dalton Trans.*, 1999, 629–634; (*c*) D.-Y. Han, Z.-P. Bai and H.-L. Chen, *Wuji Huaxue Xuebao*, 1999, **15**, 507–508; (*d*) X. Song, Y. Chen and H. Chen, *New J. Chem.*, 2001, **25**, 985–988.
12 D. Bardelang, J.-L. Clement, J.-P. Finet, H. Karoui and P. Tordo, *J. Phys. Chem. B*, 2004, **108**, 8054–8061.
13 (*a*) K. A. Connors, *Binding Constants: the measurement of molecular complex stability*, John Wiley and Sons, New York, 1987; (*b*) K. A. Connors, *Chem. Rev.*, 1997, **97**, 1325–1357.
14 H. J. Schneider, F. Hacket, V. Rüdiger and H. Ikeda, *Chem. Rev.*, 1998, **98**, 1755–1785.
15 (*a*) P. Job, *Ann. Chim. (Paris)*, 1928, **10**, 113–199; (*b*) F. Djedaïni, S. Z. Lin, B. Perly and D. Wouessidjewe, *J. Pharm. Sci.*, 1990, **79**, 643–646.
16 L. Fielding, *Tetrahedron*, 2000, **56**, 6151–6170.
17 E. A. Meyer, R. K. Castellano and F. Diederich, *Angew. Chem., Int. Ed.*, 2003, **42**, 1210–1250.
18 R. S. Macomber, *J. Chem. Educ.*, 1992, **69**, 375–378.
19 (*a*) M. Lucarini, E. Mezzina and G. F. Pedulli, *Eur. J. Org. Chem.*, 2000, 3927–3930; (*b*) A. Botsi, K. Yannakopoulou and E. Hadjoudis, *Carbohydr. Res.*, 1993, **241**, 37–46; (*c*) X. Gui and J. C. Sherman, *Chem. Commun.*, 2001, 2680–2681 and references therein.
20 M. V. Rekharsky and Y. Inoue, *Proceedings-12th International Cyclodextrin Symposium*, Montpellier, May 16–19 2004; APGI, Chatenay-Malabry, France, 2004, pp. 263–266.
21 A. Rockenbauer, T. Szabó-Plánka, Zs. Árkosi and L. Korecz, *J. Am. Chem. Soc.*, 2001, **123**, 7646–7654.

‡ CCDC reference numbers 605848 (**6d**) and 605849 (**9d**). For crystallographic data in CIF or other electronic format see DOI: 10.1039/b606062e

This journal is © The Royal Society of Chemistry 2006